

# PROTON-INDUCED CHARGE TRANSFER DEGRADATION IN CCDs FOR NEAR-ROOM TEMPERATURE APPLICATIONS

I. H. Hopkins<sup>1</sup>, G. R. Hopkinson<sup>2</sup>, and B. Johlander<sup>3</sup>

<sup>1</sup> SIRA/UCL Postgraduate Centre, South Hill, Chislehurst, Kent, BR7 5EH, UK

<sup>2</sup> Sira Limited, South Hill, Chislehurst, Kent, BR7 5EH, UK

<sup>3</sup> European Space Agency, ESTEC, Noordwijk, The Netherlands

## Abstract

An optical technique for measuring charge transfer inefficiency (CTI) in CCDs, operated under near-room temperature, high readout rate conditions, is described. It is possible to measure trap emission times and CTI dependence on signal size, background charge and clock waveform shape to high accuracy, both for serial and parallel transfers. It is shown that the presence of background charge (or 'fat zero') can substantially improve charge transfer efficiency.

## I. INTRODUCTION

During the readout of a charge-coupled device (CCD), charge is transferred in parallel from pixel to pixel down each column and then serially along an output register to an output amplifier. In this process, displacement damage-induced bulk traps within the buried channel can trap charge and release it sometime later into following charge packets - thus giving an increase in charge transfer inefficiency, CTI (the fractional charge loss per pixel transfer). Several workers [1-4] have demonstrated the effects of displacement damage on CCDs used at temperatures around -100°C and have discussed the theoretical relationships between trap capture and emission times and CTI. Low operating temperatures were used because the primary concern was the performance of spaceborne CCD-based instruments for x-ray or optical astronomy, or of detectors used in high energy physics. However the temperature range -30°C to 30°C is often more appropriate for space instruments because of design constraints (such as the need for low power consumption). Many of these instruments will also require low CTI. For instance, acquisition and tracking sensors (e.g. startrackers) need a constant optical point spread function and remote sensing instruments (such as imaging spectrometers) need accurate radiometric calibration and good resolution. In order to measure CTI for conditions relevant to these applications it has been necessary to develop an optical spot measurement technique.

A popular method of measuring low temperature CTI is to plot the intensity and location of signals produced in the CCD via illumination by x-rays from a radioactive source [1-8]. The location in the image (row and column number) gives the number of charge transfers and the intensity gives the charge loss (assuming the injected signal is always the x-ray energy divided by the 3.65eV energy needed to create an electron-hole pair). This method was extended to room temperatures

in a previous study [9]. However there are several drawbacks to this technique when used at high temperatures. Firstly the method is time consuming and applies only to some CCD architectures, since a thin epitaxial layer is needed if good 'single-pixel' x-ray events are to be obtained (an extensive field-free region below the depletion layer allows charge to spread by diffusion and these events cannot be used for CTI measurement). In addition it is desirable to vary the signal size and to measure CCDs fitted with a glass window (which will absorb x-rays of energy lower than ~10keV). Since methods such as charge injection are not applicable to most CCDs (including those discussed here), the periodic pulse technique [10] cannot be used either. Hence an optical technique was devised, involving spot illumination of the CCD followed by repeated charge transfer regimes. This is applicable to most types of CCD and gives accurate results, comparable with the x-ray method (providing that signal size, background and other measurement conditions are the same).

From Shockley-Read Hall theory (discussed in section III) we know that the emission and capture time constants ( $\tau_e$  and  $\tau_c$ ) are important parameters for a bulk trap since, for a given transfer time, they determine the fraction of traps that are unfilled and so can contribute to CTI. The capture time is not strongly temperature dependent. However the emission time varies exponentially with temperature and has a value of order 20 $\mu$ s at room temperature for the dominant proton-induced defect (the phosphorus-vacancy center). However,  $\tau_e$  is ~1 s at -90°C [2], leading to important differences between CTI behavior at 20°C compared with lower temperatures. One of the aims of this work has been to obtain an accurate measure of  $\tau_e$  for the range -20°C to 20°C.

Another important difference is that dark charge generation is higher at elevated temperatures and will usually provide a constant background charge (or 'fat zero') which helps to keep the radiation-induced traps filled. Also, higher operating temperatures are only useful in applications involving large signals. Those applications that involve signals ~1000 electrons or more, tend to be more tolerant of dark current (and associated noise sources) and so permit operation at higher temperatures. Thus the second goal was to measure the dependence of CTI degradation on background charge and signal size. It will be seen that this dependence can result in factors of 10 change in damage-induced CTI, thus explaining the CTI effects found in a previous study [9].

In order to explain the effectiveness of background charge in improving CTI, it has been necessary to re-examine the basic theory of charge trapping and in particular the

dependence on the capture time constant,  $\tau_c$ . It is well known that  $\tau_c$  is inversely proportional to signal density. In recent work ([1]-[4]) it has been assumed that the capture time is small ( a few hundred nanoseconds) and this is true for the peak signal densities encountered within the CCD buried channel. However, when present within a pixel for a longer time, charge can be captured from regions at the borders of a charge packet where the signal density is lower. In effect, this increases the volume of silicon (and hence the number of traps) involved. The result is firstly that background charge (which is present within a pixel for long periods) can fill a large number of traps and thus reduce CTI, and secondly that slow readouts (which imply that signal charge stays within a pixel for long times) produce a rise in CTI. Thus low background, low signal and slow readout conditions give a worst case for CTI. This is demonstrated by the experimental results of section IV. Note that the above remarks exclude 'freeze-out' effects which occur at low temperatures because the trap emission times are so long that traps are still full from a signal transfer by the time the next signal arrives. It should, of course, be remembered that an increased background carries the penalty of increased shot noise.

The present findings are in agreement with earlier treatments: for example Mohsen and Thompsett [10] and the somewhat neglected work of Amelio and Dyck [11] and Jack and Dyck [12]. It should also be emphasised that, with one exception, the basic conclusions of recent authors [1-4] are not in doubt, since these deal with the restricted situation of negligible background, low signals and (usually) slow transfer rates. It is only when these results are extrapolated to other conditions that errors will occur. The exception is that since the volume of silicon involved is enlarged for long pixel dwell times, the trap density has probably been overestimated, perhaps by a factor  $\sim 2$ . However this simply implies a modified value for the defect introduction rate, which in any case is not a well determined parameter.

The present results relate to standard devices without a supplementary buried channel (or 'notch'), whose purpose is to confine small charge packets within a small volume and hence improve CTI (by a factor  $\sim 3$  [6]). However the theoretical discussions could be extended to include these devices (though this would be better guided by further experimental work and is outside the scope of the present study). We note that the changes in CTI caused by variations in background, signal and transfer rate can be larger than the improvement gained by using supplementary buried channels.

## II. EXPERIMENTAL DETAILS

The CCDs were manufactured by EEV (Chelmsford, UK) and were irradiated with 10 MeV protons during the course of an earlier study [9]. The devices had 385 (horizontal)  $\times$  288 (vertical) pixels, each of area  $22\mu\text{m} \times 22\mu\text{m}$ . They had standard n-buried channels (i.e. they were not, as discussed above, of the 'supplementary buried channel' or 'notch' type). Doping in the buried channel was  $\sim 10^{16}/\text{cm}^3$ . The

irradiations were carried out at the Tandem Van de Graaff accelerator at AEA Technology (Harwell, UK) two years previously. The previous measurements [9] were made 6 months after irradiation; there was no evidence for significant annealing having taken place during the intervening period.

Test equipment, as described previously [9], consisted of an AT-compatible computer with a custom-designed programmable timing board (for generating clocking waveforms for the CCD) and a 12-bit framegrabber board (Imaging Technology Inc., VFG); a 12-bit digitizer and a specially developed software command interpreter with facilities for building automated CCD test sequences.

The optical set-up is shown in figure 1. Light from a Xenon arc passes through a green filter and is focused onto a fiber-optic cable. This routes the light to a  $12.5\mu\text{m}$  pinhole, an image of which is projected onto the CCD by a X20 microscope objective. Green light was used so that most of the absorption occurred within the depletion layer, thus avoiding lateral diffusion of photo-generated charge (which takes place in field-free regions below the depletion layer).

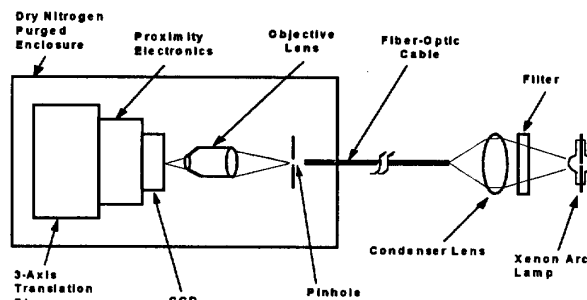


Fig. 1 Schematic diagram of the spot projection system.

The CCD and proximity electronics were mounted on a three-axis translation stage so as to remotely control the focus and position of the light spot. It was found that the spot could be projected and centered onto a pixel with less than 1% of the intensity blurred into adjacent pixels. This blurred charge acts as a small background signal but was not significant compared with the background levels used in this study (particularly as it is only present within a given pixel for one line move time - unlike dark current background which is always present). The signal amplitude of the spot was sensitive to its position relative to the electrode structure of the CCD. Some care was needed to avoid vibrations and so keep the amplitude constant. The optical bench (excluding the arc lamp) was placed inside a dark enclosure, purged with dry nitrogen gas so as to allow the CCD to be operated at temperatures below  $0^\circ\text{C}$ . Since microscope objectives can be obtained with long working distances (up to several cm) it would be possible, in an alternative arrangement, to illuminate the CCD through the window of a cryostat or other hermetic enclosure.

After integrating the signal from the spot illumination, the charge was frame-transferred into the CCD storage region, which was shielded from light. Further transfer regimes were

then carried out within the storage region to measure the emission time constant of the dominant CTI defect and the effects on CTI of dose, temperature, signal size and clock waveform. We shall call this process charge shuffling.

The parallel CTI was found by first clocking the charge in a backwards direction (away from the serial register) a total of 50 pixels, then changing direction and clocking 50 pixels back again. This movement was performed a number of times so as to achieve a large number of transfers (and so improve the accuracy). The time between line moves could be varied and, for CTI measurements, it was always ensured that time for one movement cycle back and forth was appreciably larger than the emission time constant - so that traps were empty by the time signal charge returned. Typical line move times were  $2\mu\text{s}$  at around  $15^\circ\text{C}$  and  $20\mu\text{s}$  at  $-15^\circ\text{C}$ . The CTI was found from a plot of the fractional charge loss from the spot versus the number of pixel transfers (provided that the number of transfers was not so large that a linear relation was no longer obtained). A typical plot is shown in figure 2. Serial CTI was measured in a similar way, except that charge was first transferred into the serial register before charge shuffling. The serial transfer time was  $1\mu\text{s}$  per pixel.

Background charge was provided by the dark current. Low backgrounds (down to 150 electrons/pixel at  $-20^\circ\text{C}$  after 4krad of 10MeV protons) could be achieved using a combination of fast dumping of unwanted parts of the image (to reduce the integration time) and operation with surface inversion (by dither clocking [9]). Though the latter technique only suppresses the dark current due to interface traps, and the displacement damage-induced component will limit the lowest background that can be obtained. However, it will be seen that the damage-induced CTI did not change appreciably for backgrounds below 500 electrons per pixel.

Measurements of signal and background voltages were converted to numbers of electrons using the charge to voltage conversion factor of the output amplifier, in turn measured either by using uniform illumination and monitoring the current in the amplifier reset drain, or by using  $\text{Cd}^{109}$  x-rays as a calibration source (a single pixel event produces a constant charge of roughly 6,000 electrons).

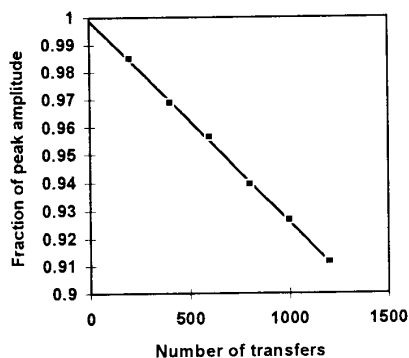


Fig 2. Typical plot of fractional charge loss versus number of pixel transfers, for spot illumination.

### III. THEORY

We assume that radiation-induced CTI in buried channel CCDs is caused by the trapping of signal charge at defect centers within the buried channel. Since the buried channel is within the depletion layer, the only important mechanisms are the capture of signal electrons from the conduction band to the trap level and their subsequent emission back to the conduction band. The time constants for these processes ( $\tau_c$  and  $\tau_e$ , respectively) are:

$$\tau_c = 1/\sigma_n v_{th} n_s \quad (1)$$

$$\tau_e = \exp(E/kT)/\sigma_n X_n v_{th} N_c \chi \quad (2)$$

where

- $n_s$  = electron density within the buried channel
- $\sigma_n$  = capture cross section for mobile electrons
- $v_{th}$  = average thermal velocity for electrons
- $N_c$  = effective density of states in the conduction band
- $T$  = absolute temperature
- $k$  = Boltzmann's constant
- $X_n$  = the 'entropy factor' associated with the entropy change for electron emission from the trap
- $\chi$  = field enhancement factor
- $E$  = energy level of the trap below the conduction band.

We have included a field enhancement factor,  $\chi$ , in the expression for  $\tau_e$  to allow for any enhanced emission due to the Poole-Frenkel effect or to phonon assisted tunneling, both of which occur in regions with an electric field greater than about  $10^4$  V/cm [13].

It can be seen that  $\tau_c$  depends on the local charge density. It is useful to distinguish between signal charge which is only found in a few sparsely separated pixels (for example signals from x-ray events, spot illuminations or from the 'highlights' of an otherwise flat image) and background charge (from dark current or a slowly varying illumination) which is present in all pixels (and is present under a storage electrode for the majority of the time). The background charge acts so as to keep a proportion of the traps in the buried channel permanently filled. Figure 3 (after [10]) shows the structure of a typical CCD and the volumes occupied by a background and a signal charge packet. A consequence of the n-buried channel structure is that there is a minimum in the electrical potential (a potential well) located about  $1\mu\text{m}$  below the silicon surface. At this location the signal density will have a maximum value. As a first approximation it can be assumed that the potential (and so  $n_s$ ) does not change much in the lateral direction until we reach the pixel edges (defined by the channel stops and the electrodes). However the signal density decreases (and  $\tau_c$  increases) rapidly for depths either side of the potential minimum. Approximations to signal density distributions have been calculated for EEV CCDs by Holland [4], Burt [14] and Robbins [15]. They are approximately gaussian with the peak electron density being proportional to total charge (signal plus background) and the  $1-\sigma$  value being approximately constant, at least for signals less than  $\sim 10^5$

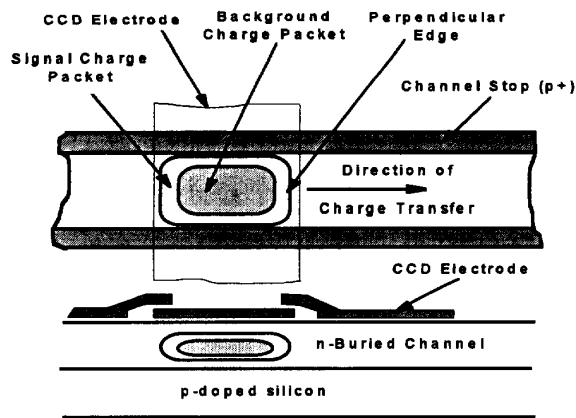


Fig. 3 Volumes occupied by a signal and a background charge packet in a buried channel CCD (after [10]). Note that, in reality, the packets do not have hard edges.

electrons (see also Mohsen and Thompsett [10]). Gaussian profiles were also assumed by Jack and Dyck [12]. In effect, the charge packets shown in figure 3 do not have sharp edges, and it will be seen that this has important implications.

It is necessary to calculate the signal charge which is trapped under an electrode. This will be zero when charge is first transferred in and will steadily increase thereafter. If  $n_t$  is the number of traps which are full (out of a total  $N_t$ ), then:

$$\frac{dn_t}{dt} = \frac{(N_t - n_t)}{\tau_c} - \frac{n_t}{\tau_e} \quad (3)$$

The solution is:

$$n_t = n_\infty [1 - \exp(-t/\tau_c) \cdot \exp(-t/\tau_e)] \quad (4)$$

where

$$n_\infty = N_t / (1 + \tau_c / \tau_e) \quad (5)$$

A steady state is reached for dwell times,  $t$ , large compared with either  $\tau_c$  or  $\tau_e$ . In a region where the signal density is low,  $\tau_c$  will be large, however the charge trapped will carry on increasing up until dwell times comparable with either  $\tau_c$  or  $\tau_e$ , whichever is the smaller. Background charge is effectively present within a pixel for the whole time it takes to transfer a frame. Hence charge can be trapped from an extended region of the buried channel where the capture time is particularly long (though the steady state fraction of traps filled will be small if  $\tau_c$  is greater than  $\tau_e$ ). It will be seen that this gives an enhanced effectiveness in the filling of traps by background charge and so a reduction in CTI.

#### IV. RESULTS

##### A. Measurements of Emission Time Constant

Because of the exponential dependence of  $\tau_c$  on energy level in equation (2) and the possibility that capture cross sections may be temperature dependent, there can be large errors in extrapolating low temperature measurements to the range of interest here (-30°C to 30°C). Hence a first step was to measure  $\tau_c$  for room temperature conditions. This was

done by repeatedly transferring the spot into an adjacent pixel, holding it there for a delay time  $\Delta t$  and then moving it back again (and waiting for  $\Delta t$ ). For delay times comparable to, or less than,  $\tau_c$  the trapped charge will not be fully emitted by the time the signal packet returns. When a steady state is reached under these conditions, all the traps within a pixel, less those which emit in a time  $\Delta t$ , will be filled. This charge will then be the amount lost from the spot. Before the steady state is reached, a smaller charge will be trapped (because some of the traps will be located in regions where the charge density is low and the capture time long). However since some of this charge remains trapped after  $\Delta t$ , the trap occupancy gradually increases until the steady state is reached. If the spot signal is  $S(\Delta t)$  ( $S_0$  without the extra transfers before readout) then:

$$S(\Delta t) = S_0 - N_t \exp(-\Delta t/\tau_c) \quad (6)$$

Note that this is not the situation described by equation (4) (which will be used in the next section) since that applies to the case where  $\Delta t \gg \tau_c$ . Now if the steady state charge lost is plotted logarithmically against delay time,  $\tau_c$  can be found from the slope of the resulting straight line. A typical plot is shown in figure 4. The emission time constant was measured for a range of temperatures between -20 and 20°C at high signal level (200,000 electrons) and backgrounds  $\sim 10,000$  electrons, with the following results:

Temp. (°C)	20	7	-5	-20
$\tau_c$ ( $\mu$ s)	22	64.5	120	430

Figure 5 shows these values plotted against  $1000/T$ . The  $T^2$  term in the ordinate follows from the temperature dependence of  $v_{th}N_c (= 4.11 \times 10^{25} (T/77)^2 \text{ cm}^{-2} \text{ s}^{-1})$  [13]. The slope of the line yields an energy level of  $0.416 \pm 0.029$  eV. The intercept, together with equation (2),  $X_n = 1.7$  and  $\chi = 1$ , gives a capture cross section ( $\sigma_n$ ) of order  $10^{-15} \text{ cm}^2$ . These values are consistent with the dominant trap defect being the phosphorus-vacancy (Si-E) center, as found by many previous workers ([3],[4],[6]). An accurate determination of  $\sigma_n$  cannot be made because of the sensitivity to the value of the trap energy level. Choosing the generally accepted value for the P-V center ( $= 0.44 \text{ eV}$ ) gives a  $\sigma_n$  of  $1.5 \times 10^{-15} \text{ cm}^2$ . The measurements were made for pixels in both parallel and serial registers with similar results. No evidence was found for significant field enhancement or for the fast traps suggested in the previous study (in a different device from the same manufacturer [9]).

Note that the values of  $\tau_c$  given above may be underestimated. This is because equation (6) is an approximation. It was found that in going to the lower temperatures (and longer delay times) the total trapped charge (which we assumed to be constant at  $N_t$ ) increased by a factor  $\sim 1.5$ . This is probably because the long delay time allows capture by a larger volume of silicon (see also figure 12). It is therefore possible that the longer times used in each  $\tau_c$  measurement also give higher charge loss.

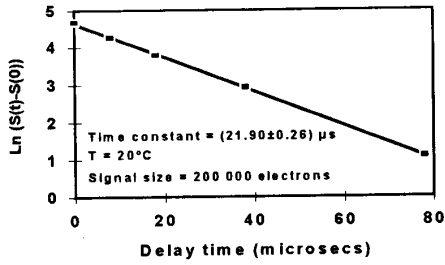


Fig. 4. The trap emission time constant is derived from plots of spot amplitude versus delay time between line moves.

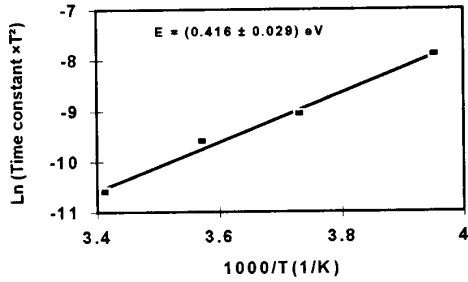


Fig. 5. Plots of  $\ln(\tau_e T^2)$  versus inverse temperature yield the energy level of the dominant trap.

This will tend to give a higher gradient in plots such as figure 4 and so an underestimated  $\tau_e$ . However allowing a factor 1.5 change in the total trapped charge only results in a 10% change in  $\tau_e$ . The above values of  $\tau_e$  are consistent with the extrapolations from the low temperature results of Robbins et al. [3] and show a greater accuracy. Measurements of charge deferred into trailing pixels are also in good agreement with these values.

**B. Effect of signal size and background on CTI**

CTI measurements were made after 4krad 10 MeV protons using the method described in section III for a variety of dark charge backgrounds and signal sizes (these could be varied separately by changing the integration time and the spot brightness). Parallel CTI was measured for a range of signals from close to full well capacity ( $\sim 3 \cdot 10^5$  electrons) down to a few hundred electrons. The errors were larger for small signal sizes but were acceptable for cases where the noise on the background was low.

The presence of a dark charge background radically affects the CTI behavior. The change in CTI with signal size, for three levels of background charge is given in figure 6, and CTI for different backgrounds at two signal sizes is shown in figure 7. It was found that for backgrounds of 500 electrons or less (the lowest value used being 150 electrons) the CTI values lay on a single curve which was a strong function of signal size, but that for backgrounds of 16,000 electrons or higher the CTI was roughly 0.00008 per pixel transfer, independent of signal size.

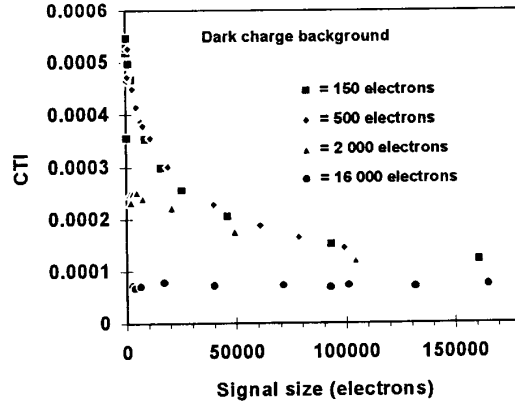


Fig. 6. CTI after 4krad 10 MeV protons for various signal sizes and backgrounds. The dwell time per phase was 0.66μs.

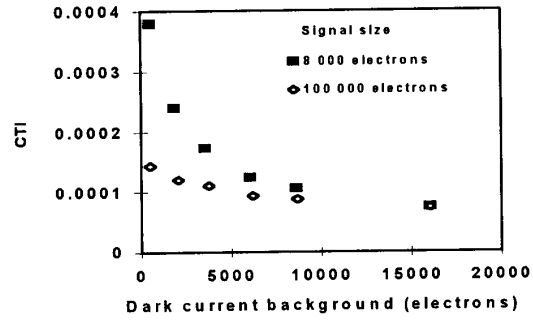


Fig. 7. As figure 6, but showing CTI versus background at two signal sizes..

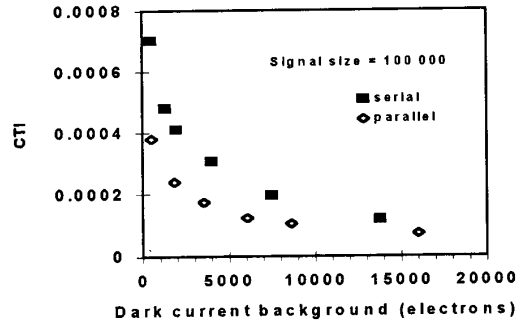


Fig. 8 Serial and parallel CTI for the same device

Measurements of serial CTI were also made. These are compared with parallel CTI in figure 8. The results converge for high backgrounds, but for low levels the serial CTI is about twice as large as the parallel. This may be related to the fact that, in these devices, the pixels in the serial register have twice the area of those in the image or storage regions.

The charge loss (= CTI x signal size) as a function of signal size is given in figure 9. This charge loss corresponds to those traps seen by the signal which have not been filled by

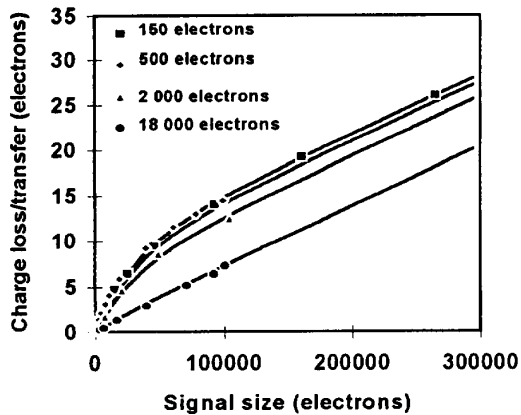


Fig. 9 Charge loss (derived from Fig. 6) versus signal size. The theoretical fit assumes that background charge is 5 times more effective in filling traps than signal.

the background charge. Assuming that the traps are evenly distributed, the charge loss corresponds to an effective extra volume occupied by the signal above that taken up by the background. It should therefore be possible to calculate the charge loss,  $\Delta q$ , for a given signal size and background from the curve for charge loss at low background. An analytical function of the form

$$\Delta q(S) = 6.6 \times 10^{-5} S + 8.5 \times \{1 - \exp(-3.15 \times 10^{-5} S)\} \quad (7)$$

was fitted to the lowest background (150 electrons) CTI data set shown in figure 9. It might be expected that the charge lost for any signal ( $S$ ) and background ( $B$ ) would be:

$$\Delta q(S,B) = \Delta q(S + B) - \Delta q(B) \quad (8)$$

However this was found to give a poor fit to the data. A much better fit (shown in figure 9 - and also fitting the data of figure 7) assumed that the background was *more effective* in filling traps than the signal - in fact by a factor 5, so that:

$$\Delta q(S,B) = \Delta q(S + 5xB) - \Delta q(5xB) \quad (9)$$

Thus, even a small background level can dramatically reduce the CTI. Reasons for this will be given below.

### C. Effect of line move rate on the trapped charge

The distribution of signal density with depth within the buried channel was discussed in section III. It has not been possible to calculate an accurate distribution, but figure 10, which is based on gaussian profiles and typical values for the peak density ([14],[15]), can be used as an illustration of roughly how the signal density varies with depth (we take it as uniform in the lateral dimensions). From these distributions the capture time can be calculated as a function of depth from equation (1). This can then be substituted in equation (4) to give the percentage of traps filled (versus

depth) for a given dwell time under an electrode (the line move time being 3 times this for a 3-phase CCD). Figure 11 shows the trap occupancy for dwell times typical of those used for signal transfer in this study, and for a longer dwell time typical of that expected for the background. The curves are for the same total charge (1000 electrons). Clearly the background fills more traps in total than the same sized signal packet and this agrees qualitatively with the results of the previous section. Using gaussian profiles does not however lead to a close fit to the data since the charge density falls too sharply - the best fit we have obtained corresponds to the empirical relation given in equation (9). It should be borne in mind that the lateral charge distribution will play a part and there will also be charge trapping in the perpendicular edges of the charge packet (figure 3). Hence a detailed model will require a three dimensional simulation of the charge distribution within the buried channel.

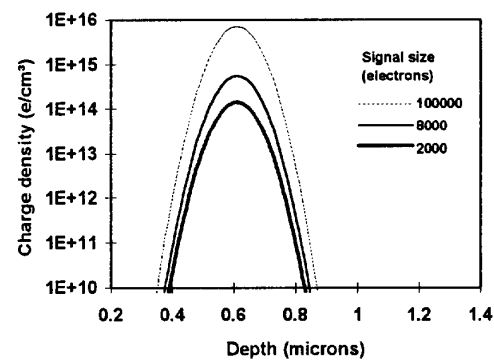


Fig. 10 Approximations to signal density distributions for different signal sizes.

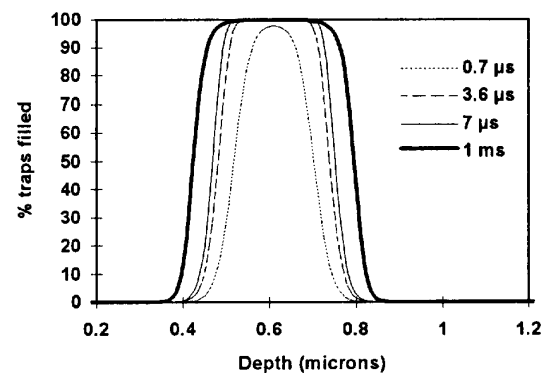


Fig. 11 Trap occupancy versus depth in the buried channel for different pixel dwell times ( $T = -10^\circ\text{C}$ )

Measurements were also made of CTI for different signal dwell times, and results are shown in figure 12. It is seen that CTI does increase as the dwell time increases, indicating that charge is indeed being trapped in a greater volume of silicon. The simple model illustrated in figures 10 and 11 predicts that the CTI saturates (i.e. ceases to increase) for dwell times

greater than  $\tau_c$ . Unfortunately the experimental conditions cannot easily cover this region because long dwell times inevitably result in high dark charge backgrounds - using lower temperatures merely increases  $\tau_c$ , so that even longer dwell times are needed. However the results of figure 12 are important since they imply that dwell times of several hundred microseconds (typical line move times for readout at  $1\mu\text{s}/\text{pixel}$ ) give a CTI increased by a factor 2 compared with line rates of a few  $\mu\text{s}$  (typical of frame transfer or fast line dump rates). Note that, depending on the clocking scheme used, the dwell time can be different for each clock phase.

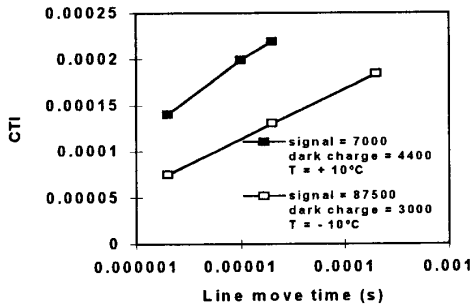


Fig. 12 CTI versus dwell time under an electrode, for constant signal size and background (electrons).

#### D. CTI versus proton fluence (or dose)

Figure 13 shows CTI versus dose (in krad(Si) - 1 krad being equivalent to  $1.8 \times 10^9$  10MeV protons/cm<sup>2</sup>). This data was obtained from different fluence regions (obtained by masking during irradiation) on each of two CCDs. High signal levels ( $\sim 10^5$  electrons) were used so that the results were not sensitive to background dark charge (which otherwise would give a reduced CTI for the higher fluence regions). Similar results were obtained in all cases and a damage factor (change in CTI per pixel transfer, divided by 10MeV proton fluence) of  $1.1 \times 10^{-14}$  cm<sup>2</sup> can be derived.

X-ray measurements using a Cd<sup>109</sup> radioactive source are given in figure 14 for the same CCDs. These correspond to signal sizes of  $\sim 6000$  electrons, but high backgrounds were used so as to minimise the effects of background variation (c.f. figure 6). Such backgrounds should give the same CTI as for the optical measurements (figure 13), if it were not for the fact that the x-ray results were obtained with frame transfer operation (and line moves every 400 $\mu\text{s}$  during readout) in contrast to the optical results for line moves every 2 $\mu\text{s}$ . It is seen from figure 12 that these differences can cause a factor  $\sim 2$  change in CTI. It is unfortunate that, due to experimental constraints, the two methods cannot be compared for exactly the same conditions; however if the differences are allowed for then the errors in either approach appear to be less than 30%. If the differences in readout and background are taken into account, the present x-ray measurements give a damage factor very similar to the value  $3.4 \times 10^{-14}$  cm<sup>2</sup> found in the previous study [5].

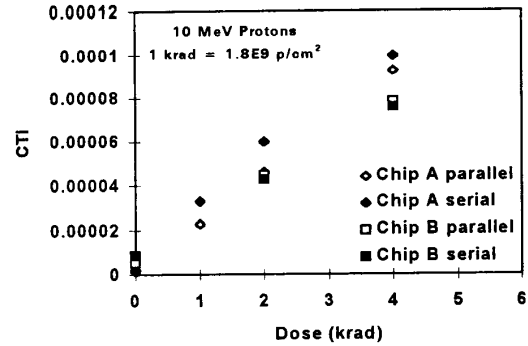


Fig. 13 Serial and parallel CTI versus dose for high signals.

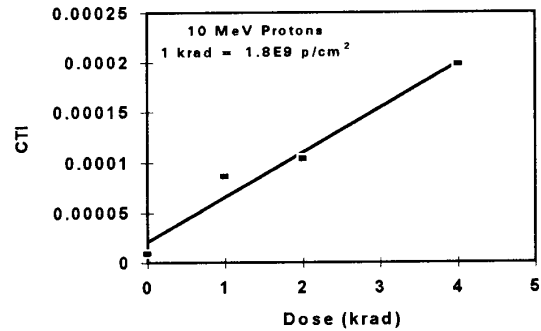


Fig. 14 X-ray results for CTI at high backgrounds.

#### E. Change in CTI with clock waveform

Though not the main object of this study, the effect of varying the clock voltages and the overlaps between clock phases was briefly investigated. It was found that clock voltage swing had little effect for serial or parallel transfers and that clock overlap had no effect for parallel transfers. However, for serial clocking, low CTI was only obtained if clock phases 1 and 2, and 3 and 1 were overlapped (the overlap between 2 and 3 not being significant). However this seems to be an effect more related to the dynamics of charge flow than to radiation damage (since the effect of proton bombardment appears to be to add a roughly constant CTI component to all the pre-irradiation measurements). Nevertheless the effect of clock waveforms on CTI is important for the design of flight electronics and it is planned to investigate this further in future.

## V. DISCUSSION

With the above results it is now possible to explain the lower CTI seen in earlier studies of CCD performance at room temperatures. The effect of background charge is to fill many of the traps within the buried channel and the reduced signal dwell times (due to faster readout, fast frame transfer or dumping) also improves CTI compared with previous low temperature measurements. Figure 6 suggests that for low

backgrounds and signal sizes the CTI damage factor for sparse signals (separated in time by more than  $\tau_c$ ) can be as high as  $7 \times 10^{-14} \text{ cm}^2$ , and allowing a factor 2 for an increased line move time in full frame readout, gives a damage factor of  $1.4 \times 10^{-13} \text{ cm}^2$  - in good agreement with low temperature, slow readout, results [1-8], but a factor 10 higher than the lowest CTI (high background) data.

However, the strong dependencies on signal size and background and the variations with signal dwell time (and, indirectly, on temperature), indicate that the prediction of CTI performance and the effect on acquired image data will not be straightforward. The ideal situation would be to have a CTI simulation model which would transport charge packets from a given scene integration through a 'virtual' CCD to give the readout image. The empirical relations (equations (7) and (9)) are a first step in developing such a model, but more work is needed. In the meantime, we make some suggestions on the prediction of CTI effects. Firstly it is necessary to classify the scene in terms of the presence of a background (perhaps slowly varying) and occasional signal 'highlights' - this is simple for star images or for x-ray events but is otherwise more complex. Also it is necessary to separate effects for different readout conditions - e.g. frame transfer or charge dumping (at typical line transfer times of a few  $\mu\text{s}$ ) or slow readout (line transfer times of a few hundred  $\mu\text{s}$ ). The charge loss can then be predicted, knowing the signal size and background. If during charge transfer the signal highlights are separated in time ( $t_0$ ) by more than  $\tau_c$  (which can be estimated from equation (2), knowing the operating temperature), then there is also a reduction in CTI by a factor  $\exp(-t_0/\tau_c)$ : this can be very beneficial at low temperatures where  $\tau_c$  is long ( $\sim 1\text{ms}$  at  $-100^\circ\text{C}$ ). The effect on the image will also depend on the spreading of the trapped charge into adjacent pixels. During frame transfer the trapped charge will usually be released over tens of trailing pixels (since  $\tau_c =$  several line times). In contrast, during readout,  $\tau_c$  can be less than the line time so that charge is only deferred to one trailing pixel.

We note that, in view of the above CTI effects, it is important when comparing data from different experiments that the experimental conditions (signal size, background, temperature and transfer rates) are carefully considered.

## VI. SUMMARY

An optical technique for measuring CTI in proton-damaged CCDs operated at room temperatures has been developed. For comparable signal and background conditions, this yields CTI and emission time constant values in good agreement with previous data. It has been shown that the presence of background charge can significantly reduce the CTI but that increasing the dwell time under each clock phase (and so the readout time) has the opposite effect. An explanation in terms of trapping in an extended region of the buried channel, where capture times are long, has been discussed. The dependence on background charge may also be important for other (lower temperature) applications.

## VII. ACKNOWLEDGEMENTS

The authors are grateful for the loan of test equipment and irradiated CCDs from the European Space Agency (ESA). This work arose partly out of a collaboration between Sira and University College London (UCL) and Alan Smith of UCL is thanked for his interest in this study. The project was funded in part by the UK EPSRC/DTI and by ESA/ESTEC.

## VIII. REFERENCES

- [1] C. J. Dale, P. W. Marshall, B. Cummings, L. Shamey and A. D. Holland, "Displacement damage effects in mixed particle environments for shielded spacecraft CCDs", *IEEE Trans. on Nuclear Science*, vol. NS-40(6), pp 1628-1637, (1993).
- [2] K. Gendreau, M. Bautz and G. Ricker, "Proton damage in X-ray CCDs for space applications: ground evaluation techniques and effects on flight performance", *Nucl. Inst. Meth.* vol. A335, pp 318-327 (1993).
- [3] M. S. Robbins, T. Roy and S. J. Watts, "Degradation of the charge transfer efficiency of a buried channel charge coupled device due to radiation damage by a beta source", RADECS 91, *IEEE Proceedings*, pp. 368-372 (1992).
- [4] A. Holland, "The effect of bulk traps in proton-irradiated EEV CCDs" *Nucl. Inst. Meth.* vol. A326, pp 335-343 (1993).
- [5] A. D. Holland, A. Holmes-Seidle, B. Johlander and L. Adams, "Techniques for minimising space proton damage in scientific charge coupled devices", *IEEE Trans. on Nuclear Science* vol. NS-38(6), pp. 1663-1670, (1991).
- [6] J. Janesick, G. Soli, T. Elliott and S. Collins, "The effects of proton damage on charge-coupled devices", in *Charge-coupled Devices and Solid State Optical Detectors II*, Proc. SPIE, Vol. 1447, pp 87-108 (1991).
- [7] B. E. Burke, R. W. Mountain, P. J. Daniels, M. J. Cooper and V. S. Dolat, "CCD soft X-ray imaging spectrometer for the ASCA satellite", *IEEE Trans. on Nuclear Science*, vol. NS-41(1), pp 375-385 (1994).
- [8] I. Zayor, I. Chapman, D. Duncan, G. Kelly and K. Mitchell, "Results from proton damage tests on the Michelson Doppler Imager CCD for SOHO", Proc. SPIE, vol. 1900, pp 97-103 (1993).
- [9] G. R. Hopkinson, "Cobalt60 and proton radiation effects on large format, 2-D, CCD arrays for an earth imaging application", *IEEE Trans. on Nuclear Science* vol. NS-39(6), pp 2018-2025 (1992).
- [10] A. Mohsen and M. F. Tompsett, "The effects of bulk traps on the performance of bulk channel charge-coupled devices", *IEEE Trans. on Electron Devices*, vol. ED-, pp (1974).
- [11] G. F. Amelio and R. H. Dyck, "Charge transport with traps", in *NATO Adv. Study Inst. on Solid State Imaging*, eds. P. G. Jespers, F. Van de Wiele and M. H. White, pp 295-304 (Noordhoff International, 1976).
- [12] M. D. Jack and R. H. Dyck, "Charge-transfer efficiency in a buried-channel charge-coupled device at very low signal levels", *IEEE Trans. on Electron Devices*, vol. ED-23(2), pp 228-234 (1976).
- [13] E. K. Banghart, J. P. Lavine, E. A. Trabka, E. T. Nelson and B. C. Burkey, "A model for charge transfer in buried channel charge-coupled devices at low temperature", *IEEE Trans. on Electron Devices*, vol. ED-38(3), pp. 1162-1174 (1991).
- [14] D. J. Burt, private communication (1994).
- [15] M. Robbins, "Radiation Damage Effects in Charge Coupled Devices", PhD. Thesis, Brunel University (1992).